RESEARCH ARTICLE

Lung epithelial cells have virus-specific and shared gene expression responses to infection by diverse respiratory viruses

James T. VanLeuven[1], Benjamin J. Ridenhour[1,2], Andres J. Gonzalez[1,2], Craig R. Miller[1,2,3], Tanya A. Miura[1,2]*

1 Center for Modeling Complex Interactions, University of Idaho, Moscow, Idaho, United States of America,
2 Department of Biological Sciences, University of Idaho, Moscow, Idaho, United States of America,
3 Department of Mathematics, University of Idaho, Moscow, Idaho, United States of America

* tmiura@uidaho.edu
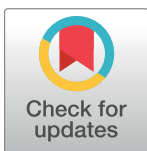
Abstract

The severity of respiratory viral infections is partially determined by the cellular response mounted by infected lung epithelial cells. Disease prevention and treatment is dependent on our understanding of the shared and unique responses elicited by diverse viruses, yet few studies compare host responses to viruses from different families while controlling other experimental parameters. Murine models are commonly used to study the pathogenesis of respiratory viral infections, and *in vitro* studies using murine cells provide mechanistic insight into the pathogenesis observed *in vivo*. We used microarray analysis to compare changes in gene expression of murine lung epithelial cells infected individually by three respiratory viruses causing mild (rhinovirus, RV1B), moderate (coronavirus, MHV-1), and severe (influenza A virus, PR8) disease in mice. RV1B infection caused numerous gene expression changes, but the differential effect peaked at 12 hours post-infection. PR8 altered an intermediate number of genes whose expression continued to change through 24 hours. MHV-1 had comparatively few effects on host gene expression. The viruses elicited highly overlapping responses in antiviral genes, though MHV-1 induced a lower type I interferon response than the other two viruses. Signature genes were identified for each virus and included host defense genes for PR8, tissue remodeling genes for RV1B, and transcription factors for MHV-1. Our comparative approach identified universal and specific transcriptional signatures of virus infection that can be used to distinguish shared and virus-specific mechanisms of pathogenesis in the respiratory tract.

Introduction

Viruses from several different families, including *Picornaviridae*, *Orthomyxoviridae*, *Paramyxoviridae*, *Coronaviridae*, and *Adenoviridae*, infect and cause diseases in the respiratory tract. These diseases range from mild infections of the upper respiratory tract, to severe diseases when viruses infect the lungs. Respiratory viruses commonly target epithelial cells of the

airways and lungs. These epithelial cells are responsible for detecting viral pathogens and initiating antiviral responses at the level of infected cells and the immune system, and therefore their response to infection has an important role in determining disease outcomes. Knowledge of the shared and virus-specific responses of respiratory epithelial cells to infection by diverse viruses is fundamental to understanding viral pathogenesis and developing therapies to treat severe respiratory infections.

Murine models of respiratory viral infections have been widely used to identify the mechanisms that determine disease severity in the respiratory tract. While these models are invaluable for evaluating pathology and host responses to infection, parallel *in vitro* studies can be used to identify gene expression and signaling pathway changes that occur in infected cells to mediate pathogenesis. In this study, we compare the gene expression response of murine lung epithelial cells to infection by three respiratory viruses used in murine models: rhinovirus (serotype RV1B) in the family *Picornaviridae*, mouse hepatitis virus (MHV strain 1) in the family *Coronaviridae*, and influenza A virus (strain PR8) in the family *Orthomyxoviridae*. Viruses from different families and with different replication strategies were chosen to identify which responses to infection in respiratory epithelial cells are shared and which are virus-specific. In the following paragraphs, we describe some of the key features of these three viruses in murine models.

Minor group rhinoviruses, including RV1B, use low-density lipoprotein receptor to enter either human or murine cells. Because RV1B can replicate in mouse cells, it has been used to study immune responses and mechanisms of asthma exacerbation in infected mice [1–5]. Intranasal inoculation of mice with a high dose of RV1B results in viral replication and an early inflammatory response in the respiratory tract without clinical signs of disease [1, 3–5]. RV1B antigens have been detected in cells of the epithelia and lamina propria of the upper respiratory tract of infected mice [2, 4].

MHV-1 is a strain of mouse hepatitis virus that preferentially replicates and causes disease in the respiratory tract of specific mouse strains and thus serves as a model for respiratory coronaviral infections [6, 7]. MHV-1 causes severe disease in A/J-strain mice and milder pathology in other mouse strains [6, 8]. Mouse strain-dependent disease severity corresponds to inflammatory responses, fibrin deposition, and reduced type I interferon (IFN) production [6]. Further, type I IFN-mediated signaling is required for protection from severe disease during MHV-1 infection of resistant mice [8]. MHV-1 has been detected in pulmonary macrophages of infected mice, but has not been reported to infect respiratory epithelial cells *in vivo* [6]. Although primary murine alveolar epithelial cells are susceptible to MHV-1 infection *in vitro*, their role during *in vivo* infection is not clear [9].

Mice have been used for decades to study the pathogenesis of influenza. One of the most commonly used strains of influenza A virus, PR8, has been serially passaged in mice to produce a model for pulmonary infection. PR8 infection results in a range of disease severities that is mouse strain-dependent [10]. Although susceptible mice mount a type I IFN response to PR8 infection, lethal infection is associated with spread of virus to the alveoli and an excessive inflammatory response [10–13]. PR8 replicates in bronchiolar and alveolar epithelial cells of the lower respiratory tract *in vivo* and in primary murine respiratory epithelial cells *in vitro* [9, 12, 14, 15].

In this study, we used a murine lung epithelial cell line (LA4) to compare the gene expression response to these three unrelated viruses. LA4 cells were derived from neoplastic lung epithelia from strain A (A/He) mice and have some properties of alveolar type II cells, although they do not maintain a highly differentiated type II phenotype [16]. Strain A (A/J) mice are highly susceptible to respiratory viral infections, including MHV-1 and influenza A viruses [6, 10]. Other studies have demonstrated that LA4 cells are susceptible to infection by PR8 and

RV1B [15, 17]. In this study, we show that LA4 cells are also susceptible to infection by MHV-1 (hereafter referred to as MHV). The gene expression response of LA4 cells to infection by MHV, PR8, and RV1B (hereafter referred to as RV) differed in timing and magnitude of the changes. While we expected to see highly divergent transcription responses to these three viruses, they induced expression of a surprisingly large overlapping set of shared genes, including genes involved in antiviral responses. However, and more in line with our expectation, each virus also altered expression of unique genes, which highlight their different replication strategies and mechanisms of pathogenesis in murine hosts.

Materials and methods

Virus stocks and cell lines

Virus stocks were generated by 24 h of growth from a low dose inoculum in the cell lines described below. Supernatant medium from infected cells was centrifuged to remove cell debris, aliquoted, flash frozen and stored at -80°C. PR8 (A/Puerto Rico/8/1934 (H1N1)), obtained from BEI Resources (NR-3169), was grown and titrated by plaque assay in MDCK cells from ATCC (CCL-34) [18]. MHV, obtained from ATCC (VR-261), was grown and titrated by plaque assay in 17Cl.1 cells [19] (provided by Dr. Kathryn Holmes, University of Colorado Denver School of Medicine). RV, obtained from ATCC (VR-1645), was grown and titrated by tissue culture infectious dose 50% ($TCID_{50}$) assay in HeLa (ATCC: CCL-2) cells [17]. LA4, a murine lung epithelial cell line from ATCC (CCl-196), was cultured in Ham's F12K medium (Mediatech) with 10% FBS (Atlanta Biologicals) and 1X antibiotic/antimycotic (Gibco).

Epithelial cell infection and microarray sample

Our experimental approach was to inoculate LA4 cells with the three viruses at times t = 0 h and t = 12 h and harvest RNA for microarray analysis at t = 24 h. Controls were mock-inoculated at both time points. Preliminary experiments were done to establish the growth kinetics of each virus and determine a multiplicity of infection (MOI) that resulted in comparable numbers of cells positive for viral antigen at 24 h post-infection (S1 Fig). Based on this, LA4 cells were inoculated with 3 $TCID_{50}$/cell RV, 1 PFU/cell PR8, or 3 PFU/cell MHV. Triplicate wells of LA4 cells in 6-well plates were inoculated with each virus diluted in serum-free medium or were mock-inoculated with serum-free medium for 1 h at 37°C. Viral inocula were removed and the cells were rinsed twice with serum-free medium. The cells were incubated in Ham's F12K medium with 2% FBS until the 24 h time point at which time RNA was isolated from cell cultures using an RNAeasy Plus kit (QIAGEN) and transcript levels were measured by microarray (NimbleGen *Mus musculus* MM9 Expression Array). For the 24 h samples, the media were removed and replaced with fresh media 12 h after inoculation, which is the same time that 12 h samples were inoculated. Raw and processed data are available from NCBI Gene Expression Omnibus under accession number GSE89190.

Data analysis

NimbleScan v2.5 software (NibleGen, Madison, WI) was used to extract raw intensity data for each probe on each array. Intensity data were read into the R statistical computing environment and checked for quality [20]. Data were prepared for processing using the pdInfoBuilder package and then normalized using the robust multichip average (RMA) function in the oligo package [21].

Statistical tests for differences in expression between treatments were conducted on the normalized expression data using a linear mixed-effect model followed by linear contrasts corrected for multiple comparisons. More specifically, expression was modeled as a function of treatment, while probes for a particular gene were treated as random effects. The models used the nlme::lme function in R. The data contained seven treatments: three viruses tested at two time points (12 h and 24 h) each plus the mock treatment (RV_{12}, RV_{24}, MHV_{12}, MHV_{24}, $PR8_{12}$, $PR8_{24}$, and mock). The following nine post hoc, two-sided contrasts were then performed on the fitted models using the multcomp::glht function in R: each virus-time combination vs. mock (RV_{12} vs. mock, RV_{24} vs. mock, MHV_{12} vs. mock, MHV_{24} vs. mock, $PR8_{12}$ vs. mock, $PR8_{24}$ vs. mock) and each pairwise combination of viruses at the 24 h time point (RV_{24} vs. MHV_{24}, RV_{24} vs. $PR8_{24}$ MHV_{24} vs. $PR8_{24}$). These 9 tests had their p-values adjusted by the multcomp::summary.glht function according to their joint distribution. Any factors detected to be significant at the family (gene) level were then subsequently corrected using the Benjamini-Hochberg algorithm [22] with a false discovery rate set at 1%.

Genes associated with type I IFN responses were identified among the sets of genes with differential expression for each virus compared to mock at 12 h and 24 h using the Interferome v.2.01 database (http://interferome.its.monash.edu.au; [23]). This database was queried using the search criteria: Type I IFN (all), *in vitro*, *Mus musculus*, 2.0 fold change (up or down). Interferome genes were manually sorted into functional categories: antiviral, IFN signaling, viral detection, immune response, MHC class I, inhibitory, apoptosis, ubiquitination, miscellaneous, and unknown. The significance of each virus having genes in the specific categories was tested using a chi-squared test.

Gene expression responses to RV1B were compared between our data from mouse cells and published data using human cells [24] using the MGI vertebrate homology database provided by The Jackson Laboratory [25] as well as the annotate package in R.

Results and discussion

MHV, PR8, and RV alter cellular gene expression by different magnitudes and with different timing

Our goal was to evaluate the gene expression response of murine respiratory epithelial cells to infection by three unrelated respiratory viruses studied in murine models. A preliminary study was undertaken to identify a murine cell line that was susceptible to infection by the three viruses. LA4 cells were chosen because MHV, RV, and PR8 established productive infections in this line, as shown by increased viral titers released from infected cultures over a 24 h infection (S1 Fig). Additionally, comparable numbers of viral antigen-positive cells were observed for the three viruses 24 h after inoculation of LA4 cells (S1 Fig).

To compare how unrelated respiratory viruses (MHV, PR8, and RV) alter gene expression of murine epithelial cells, we inoculated LA4 cells with each of the three viruses and evaluated cellular gene expression by microarray analysis after 12 and 24 h of infection compared to mock-inoculated controls. Fig 1 shows the log_2-fold change in expression level of genes that were differentially expressed in virus-infected, compared to mock-inoculated, cells. By plotting the changes in gene expression at 12 vs. 24 hours, we observed differences in magnitude and timing of gene expression changes mediated by the three viruses. The genes with significantly different expression in MHV-infected cells had low fold change values (Fig 1A). At 24 h, when gene expression changes were the highest, genes that were up-regulated by MHV infection had log_2-fold change values of less than five. In contrast, PR8 and RV induced expression of many genes by greater than five log_2-fold at 24 h, and genes were spread consistently across the full range of values. By 24 h, the genes most strongly up-regulated by PR8 and RV induced changes
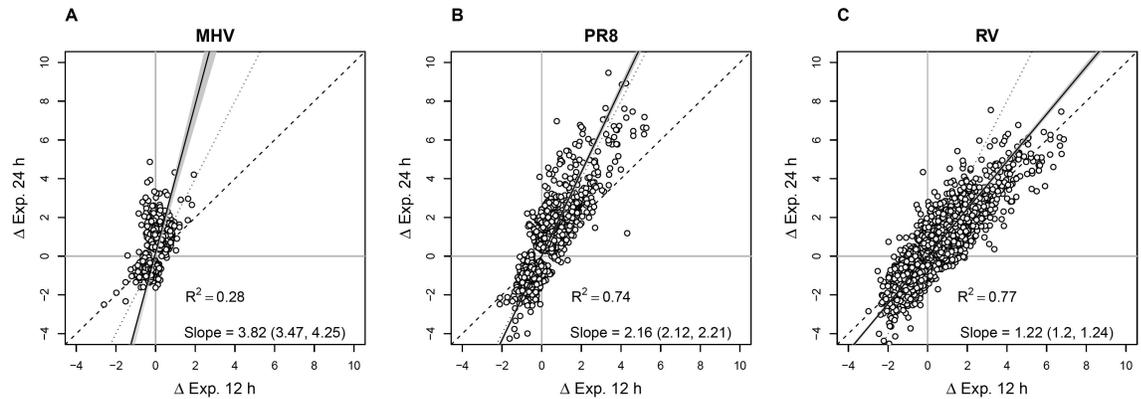
Fig 1. Magnitude and timing of gene expression changes mediated by MHV, PR8, and RV. The plots show the estimated $\log_2$-fold change in expression relative to mock at 12 h vs. 24 h for each virus. Each point represents one gene; only those genes that differ significantly from mock (at either time point) are included. The solid black line is the best fit regression line with the gray shading showing the 95% confidence interval. The slope with confidence interval and R^2 are given in the inset legend. The dashed line illustrates the hypothesis that all changes in expression occur in the first 12 h (slope = 1); the dotted line shows the constant rate of change hypothesis (slope = 2). **(A)** MHV has small effects and most of the expression changes occur between 12 and 24 h (slope >> 2). **(B)** PR8 has larger effects than MHV and the changes approximate a constant rate of change across both 12 h intervals (slope $\approx$ 2). **(C)** RV also has large effects on gene expression and changes occur in the first 12 h with very little further change in the next 12 h (slope $\approx$ 1).

https://doi.org/10.1371/journal.pone.0178408.g001

of 7–9.5 $\log_2$-fold and 6–7.5 $\log_2$-fold compared to mock, respectively. This same pattern was observed with the down-regulated genes (Fig 1).

In addition to the differences in fold change values, the three viruses also differed in the timing of gene expression changes. MHV altered expression of relatively few host genes, most of which were only significantly different from mock at 24 h (Fig 1A). While both PR8 and RV induced expression of large subsets of host genes, they did so with different timing. PR8-induced changes in gene expression occurred at a constant rate: the expression level of most genes at 24 h was approximately twice the expression value at 12 h (Fig 1B). In contrast, RV infection altered expression of a large number of genes by 12 h and the expression levels were maintained at approximately the same levels at the 24 h time point (Fig 1C).

Taken together, we observed differences in magnitude and timing of gene expression changes mediated by the three viruses. The limited response to MHV infection is in agreement with studies of other coronaviruses, such as MHV-A59 [26] and SARS-CoV [27, 28]. In addition to inducing minor transcriptional up-regulation of host genes, MHV-A59 shuts down host gene expression by enhancing mRNA degradation [26]. A related coronavirus, SARS-CoV, also induces degradation of host mRNAs [29]. The low numbers of host mRNAs that were altered in response to MHV infection in our study could be due to one or both of these mechanisms. While rhinoviruses are known to down-regulate host gene expression by inhibiting transcription [30], upon RV infection we saw robust, early increases in host mRNA expression (Fig 1C). This is in agreement with other transcriptome studies of major and minor serogroup rhinoviruses in human respiratory epithelial cells and experimental infections of humans [24, 31–34]. The plateau in gene expression changes in RV-infected cells at 24 h may be due to transcriptional inhibition later in infection, or the death of infected cells. PR8 infection induced a strong transcriptional response in LA4 cells, which has also been seen with multiple strains of influenza A viruses in primary human and mouse airway or lung epithelial cells [35–38].

Interestingly, the differences in kinetics of host cell gene expression did not correspond with differences in the kinetics of viral replication in this cell line (S1 Fig). Despite inducing

expression of a large number of host genes by 12 h post-infection, infectious RV was not released from the LA4 cells until after the 12 h time point. In contrast, the titers of MHV and PR8 in the medium of infected cells increased by the 12 h time point (S1 Fig). However, the gene expression responses to MHV and PR8 increased from 12 h to 24 h post-infection (Fig 1). These data also demonstrate that the limited response of cellular gene expression to MHV infection was not due to limited infection of LA4 cells (S1 Fig).

Host genes have shared and unique responses to RV, PR8, and MHV infection

We identified which genes were altered by each virus at 24 h compared to mock and the degree of overlap among the differentially expressed genes. At 24 h RV infection resulted in up-regulation of the largest number of genes, followed by PR8 then MHV (Fig 2A); a similar pattern was seen with down-regulated genes (Fig 2B). While one might worry that some of the small number of significant genes that were altered by MHV could be false positives, the majority of these genes (65% of up-regulated and 86% of down-regulated genes) were also significantly altered by at least one other virus suggesting that most of these genes are true positives. For both up- and down-regulated gene sets, RV had the largest proportion of unique genes, while the majority of genes affected by PR8 and MHV were shared by at least one other virus.

S1 Table contains the list of genes whose expression was significantly up-regulated by all three viruses compared to mock-inoculated cells. These genes may reflect a global response of epithelial cells to viral infection. Several of the genes with the highest fold change values are involved in antiviral defense at the level of infected cells (eg., *Mx1, Bst2, Oas2, Gbp10*) or recruitment of immune cells (eg., *Cxcl10, Cxcl11, Cxcl1*). These genes are up-regulated by type I IFNs, suggesting that induction of a type I IFN response is shared by these viruses. In contrast to the shared up-regulated genes, genes that were significantly down-regulated by all three viruses have diverse functions (S2 Table). Some examples of genes that were down-regulated by all three viruses included genes that encode transmembrane proteins (*Tmem 119, 231, 19, 50a,* and *14c*), extracellular matrix proteins (*Spon2, Ogn, Aspn*), and apoptotic signaling proteins (*Sdpr, Bmf, Bnip3l*). As a measure of validation, the expression levels of five genes (*Tnf,*
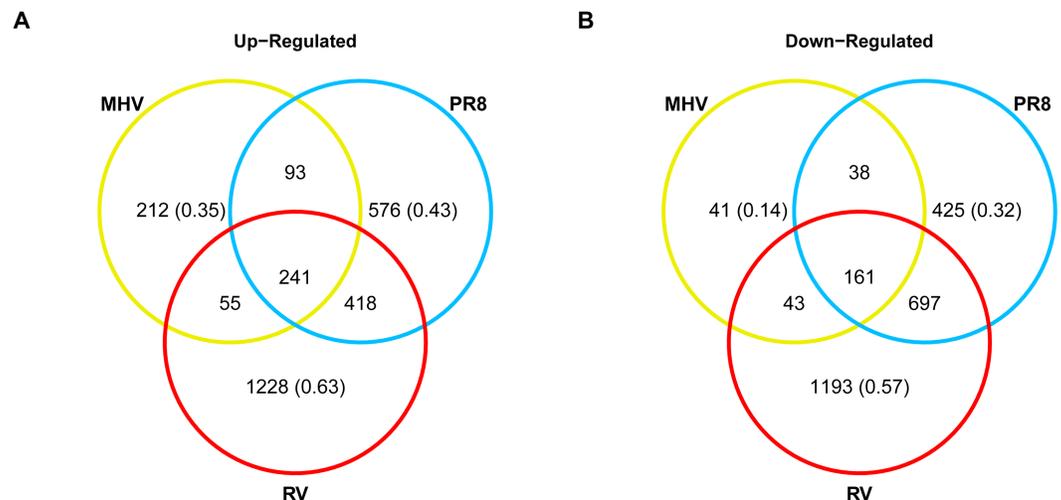
Fig 2. Numbers of genes with significantly altered expression upon viral infection. Venn diagrams show the number of significantly **(A)** up- and **(B)** down-regulated genes compared to mock 24 h after infection. The proportion of genes that are uniquely significant for each virus is indicated in parentheses.

https://doi.org/10.1371/journal.pone.0178408.g002

Cxcl10, *Bst2*, *Icam1*, and *Oas1a*) were also quantified by RT-qPCR at 24 h post-infection (S2 Fig). A strong correlation was observed between RT-qPCR and microarray measurements of gene expression (slope = 1.02, R^2 = 0.87).

Identification of signature genes that were uniquely altered by each virus

Comparing the number of genes altered by each virus provides insight into shared and unique cellular responses elicited by the viruses, but it does not provide information on the relative magnitudes of gene expression changes between viruses. To compare gene expression changes between viruses, we plotted the log_2-fold change of each gene at 24 h for MHV vs. RV vs. PR8 (Fig 3A). We only included genes that were differentially expressed in at least one viral infection compared to mock. Like Fig 1, this 3D plot illustrates that PR8 and RV not only caused a larger number of genes to be up-regulated compared to MHV, but they also induced higher fold change values (Fig 3A).

For each of the three viruses, we defined a signature gene as a gene that is both differentially regulated at 24 h compared to the mock treatment and has an effect size significantly larger than the other two viruses (i.e. fold change on the X axis is significantly different from Y-axis, Z-axis, and mock). These genes are colored in Fig 3A and appear along the diagonal in Fig 3B. As expected, RV had the largest number of signature genes, followed by PR8, then MHV (Fig 3B). Interestingly, the genes with the highest fold change values compared to mock were not signature genes, but were up-regulated by both PR8 and RV infection. A pairwise analysis was performed to identify the number of genes with altered expression compared with mock in two viruses compared with the third. This analysis, shown in Fig 3B, reveals that RV and PR8 had the most similarities in both up- and down- regulated genes (Fig 3B, purple blocks). The
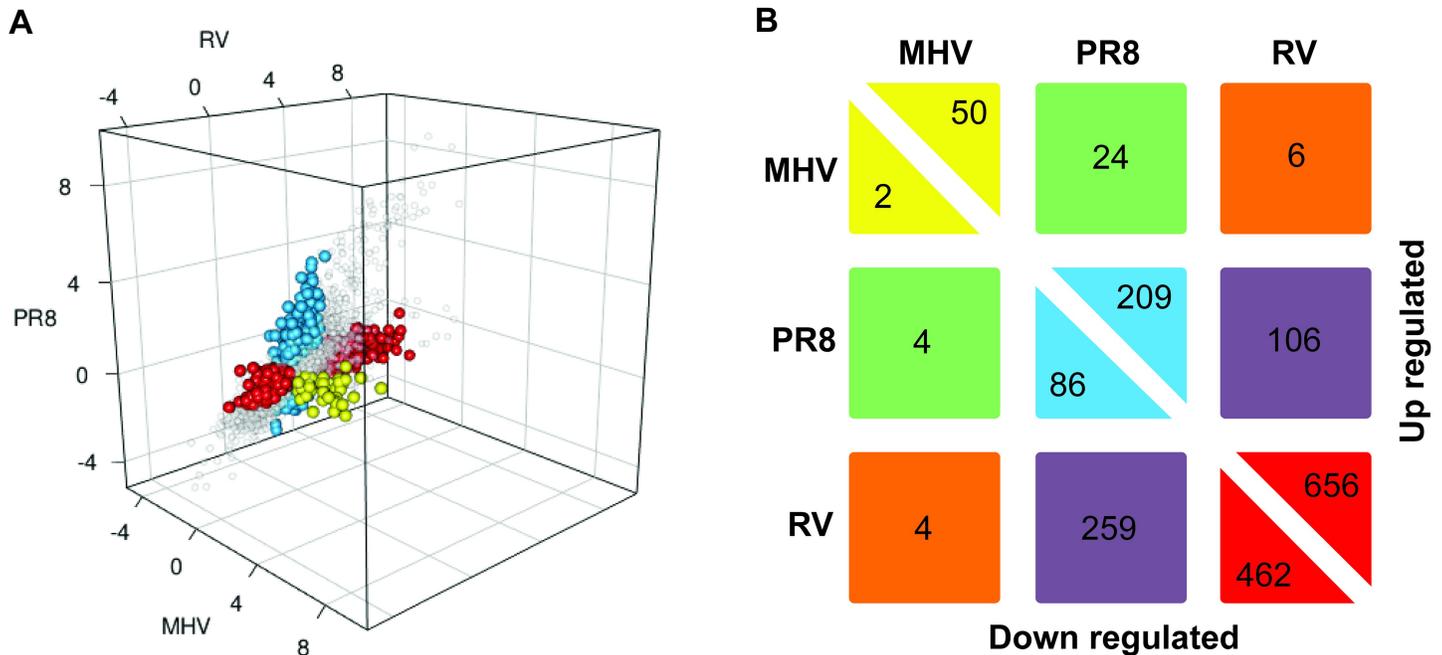
Fig 3. Patterns of gene expression changes mediated by viral infection. (A) Genes differentially expressed in at least one viral infection at 24 h are plotted as log_2-fold change with each virus along a different axis. Signature genes, which have significantly larger effects in one virus compared to all other treatments, are colored: blue = PR8, red = RV, yellow = MHV. **(B)** The number of genes uniquely up- or down- regulated by each virus or pairs of viruses. The numbers along the center diagonal are the signature genes with boxes colored as in (A). The off-diagonal numbers are genes that have differential expression in two viruses compared to mock and the third virus, but are not significantly different from each other.

pattern of up-regulated gene expression changes during MHV infection was more similar to PR8 (24 genes) than RV (6 genes). This may reflect the fact that PR8 and MHV cause severe pathogenesis in mice, whereas RV-infected mice do not exhibit clinical signs of disease. Among the six genes co-upregulated by MHV and pR8 was TNF-α, a key proinflammatory cytokine (not shown).

Several host defense genes were identified as signature genes uniquely up-regulated by PR8 infection (S3 Table). These genes included cytokines and chemokines (*Cxcl9*, *Ccl5*, *IL12b*, *Ccl8*), IFN response genes (*Ifitm6*, *Ifi27l2a*, *Ifna2*, *Ifit2*, *Ifitm5*, *Ifna11*), and genes involved in processing MHC class I antigens (*Psmb10*, *Tap2*, *H2-Q2*, *H2-K1*, *Psmd9*, *Psme2*, *Psme1*). The significant up-regulation of host defense genes in response to PR8 in the LA4 cell line corresponds with the expression profile of murine type II alveolar epithelial cells in response to PR8 infection in mice [39]. PR8 infection in highly susceptible mouse strains results in dramatic up-regulation of inflammation-associated genes when compared to resistant mouse strains [11]. Many studies in murine models of influenza A virus infection have demonstrated a relationship between an excessive inflammatory response and disease severity [10–12, 15]. Furthermore, infection of TLR3-/- mice with influenza A virus results in a reduced inflammatory response and increased survival [40]. Our data support the role of alveolar epithelial cells in generating this excessive inflammatory response *in vivo*. Several genes that were uniquely down-regulated by PR8 are involved in cellular metabolic pathways (*Cdo1*, *Aldh1a7*, *Acad11*, *Hsd17b4*) or intracellular transport (*Myl6b*, *Ift88*, *Anxa8*).

Although RV induced expression of several genes involved in host defense, these were largely shared by PR8 so were not identified as signature genes. The signature genes up-regulated by RV included kallikrein-1 and ten kallikrein-1-related peptidases and additional proteins involved in tissue remodeling (S4 Table). Although tissue remodeling is not likely to be relevant in murine models of rhinovirus infection alone, due to the limited damage, it may be an important factor in murine models of rhinovirus-induced allergic asthma [1, 2, 41]. Rhinovirus infections are a significant cause of asthma exacerbations, which correspond with inflammatory responses in the airways. Kallikreins generate kinins and contribute to many disease processes, including inflammation. Kinins are induced by rhinovirus infections and kallikrein-1 is up-regulated by rhinovirus infection in humans, especially those with asthma [42, 43]. Up-regulation of these genes in mouse cells upon RV infection would provide a tractable animal model in which to study the roles of kallikreins in rhinovirus-induced asthma exacerbations. Mucins, which contribute to mucus hypersecretion, are up-regulated by rhinovirus infection of airway epithelial cells *in vitro* and in mice [1, 44]. *Muc2* was the only mucin gene up-regulated by RV in our study, and was unique to RV infection (S4 Table).

MHV infection resulted in regulation of a small set of signature genes (Fig 3B, S5 Table). Signature genes that were uniquely up-regulated by MHV infection included multiple transcription factors from the double homeobox (*Duxf3*, *Dux*, *Dux4*) and zinc finger and SCAN domain (*Zscan4d*, *Zscan4c*, *Zscan4-ps1*, *2 and 3*) families. Despite up-regulating expression of transcription factors, MHV infection had a minor impact on the host cell transcriptome. This may be due to enhanced degradation of mRNAs as discussed above, which has been shown to occur during other coronaviral infections [26, 29]. Therefore, LA4 cells may be up-regulating transcription in response to MHV infection through expression of various transcription factors while MHV causes degradation of these transcripts, which would reflect the small number of up-regulated transcripts in MHV infected samples. In contrast to MHV-A59, MHV-1 infection did not cause down-regulation of a substantial number of host genes. Differences could be due to virus strain, host cell type, and timing differences between the studies. In contrast to the robust up-regulation of genes involved in innate immunity and inflammatory responses by PR8 and RV, the limited response of infected epithelial cells to MHV infection may reflect the

ability of MHV to replicate (S1 Fig) without being detected by the host cell. Coronaviruses, including MHV, delay induction of antiviral responses. Multiple mechanisms have been proposed to account for this, including replicating within double membrane vesicles, ribose 2'-O-methylation of viral mRNA, and endonuclease activity within the RNA polymerase complex [45–48]. This would allow MHV to replicate to higher levels before triggering antiviral defenses, which might promote pathogenesis in the murine respiratory tract [6]. Alternatively, the reduced response to MHV by epithelial cells may reflect the different cellular tropism of MHV. In contrast to PR8 and RV, which are known to infect epithelial cells in the murine respiratory tract, MHV-1 has only been reported in alveolar macrophages [2, 6, 12].

Type I IFN-related genes had increased expression in LA4 cells infected by PR8, RV, and MHV

As described above, several of the genes with up-regulated expression in response to all three viruses, as well as those that were unique to PR8, are induced by type I IFNs. To specifically evaluate how IFN response genes were altered by the three viruses, genes that were significantly up-regulated by each virus at the 24 h time point were used to query the Interferome v2.01 database (see Materials and Methods). A Venn diagram was generated to visualize the degree of overlap in IFN-related genes whose expression was induced by at least one of the three viruses (Fig 4). PR8 induced expression of the greatest number of IFN-related genes, a majority of which were shared by at least one other virus. RV up-regulated slightly fewer IFN-induced genes compared to PR8 and MHV infection resulted in up-regulation of the fewest IFN-induced genes. It was somewhat surprising that PR8 induced a higher type I IFN response than RV, given that RV induced expression of nearly twice as many genes than PR8 (Fig 2). However, some of these genes contribute to inflammatory responses, which could explain the excessive inflammatory response to PR8 infection vs. the self-limited inflammation during RV infection in mice [10–12, 15].

There was strong overlap between the IFN-induced genes up-regulated by each virus. The timing of IFN-related gene expression followed the same trend as was seen for all significant genes in Fig 1 (data not shown). Most of the IFN-related genes up-regulated by MHV were only increased at 24 h. PR8 induced expression of 110 IFN-related genes at 12 h and these genes were a subset of the 179 genes up-regulated at 24 h. In contrast, RV infection induced expression of more IFN-related genes at 12 h (148 genes) than at 24 h (123 genes). Relative to up-regulation, few IFN-related genes were down-regulated at the 24 h time point (MHV = 5, PR8 = 10, RV = 26).

Type I IFNs induce expression of genes with different functions during an antiviral response. To determine whether there were specific patterns in expression of IFN-induced genes that correspond with function, the IFN-induced genes that had significantly increased expression by any of the three viruses were separated into functional groups. Heatmaps that demonstrate differences in fold change (color scale) and significant differences (outlined boxes) in expression compared to mock-inoculated controls were generated (Figs 4 and S3). As shown in the Venn diagram, this analysis also demonstrates that PR8 infection resulted in up-regulation of the most genes involved in type I IFN responses, followed by RV then MHV. The fold change values induced by PR8 infection were also generally higher than the other two viruses. However, there was not a significant association between virus identity and functional group. For most of the functional groups, MHV up-regulated expression of a smaller subset of the same genes as PR8 and RV, with the exception of the MHC class I pathway (Fig 4). MHV significantly up-regulated expression of only one gene involved in the MHC class I pathway (*Blmh*), which was not significantly up-regulated by the other two viruses. This observation
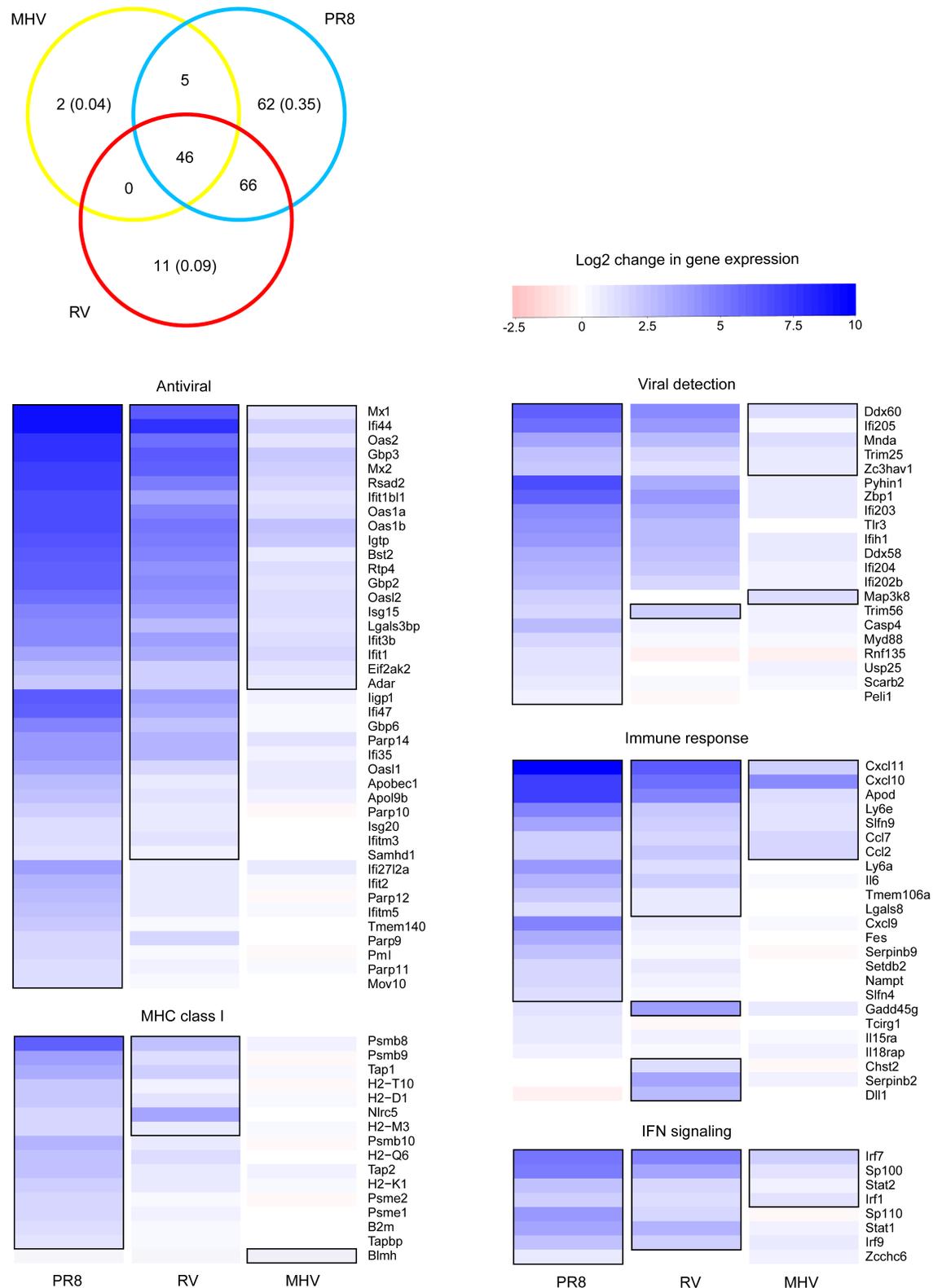
Fig 4. Differential expression of type I interferon-induced genes. Genes with significantly up-regulated expression compared to mock at 24 h (see Fig 2) were used to query the Interferome v.2.01 database. The Venn diagram shows the number of shared and unique type I IFN-related genes that were up-regulated in each viral infection. The proportion of

genes up-regulated in only one virus treatment are shown in parentheses. The genes represented in the Venn diagram were divided into functional groups and heat maps were generated using $\log_2$-fold change values for each virus at 24 h compared to mock-inoculated controls. Heat maps of additional functional groups can be found in S3 Fig. Gene names are indicated to the right of each row and statistically significant values are outlined in black.

suggests that cytotoxic T cell responses may differ in MHV infections compared to PR8 and RV. T cell responses have complex roles in MHV-1 infections, as they contribute to protection in resistant mouse strains but mediate pathology in susceptible strains [49]. However, mice with the CD8+ T cell repertoire of a resistant strain in the background of a susceptible strain remain susceptible to severe MHV-1 infection [50]. The failure of MHV-1 to activate processing and presentation of MHC class I antigens could explain the inability of a broadly reactive CD8+ T cell response to protect these mice.

The interferome analysis focuses on IFN-induced gene expression, but not expression of the type I IFNs that induce these responses. Multiple type I IFNs exist, including IFN-β and 14 subtypes of IFN-α, all of which signal through the type I IFN α/β receptor [51]. Type I IFNs can induce autocrine and paracrine signaling; thus the IFN-induced genes we detected could be from both infected and uninfected cells in the cultures. To determine if differential expression of type I IFNs explains the differences in IFN-induced gene expression upon infection by PR8, RV, and MHV, we analyzed the expression of type I IFN and receptor genes for each virus compared to mock (Fig 5). Probes for IFN-β1 and ten subtypes of IFN-α were present on the arrays. In agreement with expression of IFN-induced genes, PR8 induced expression of the largest set of type I IFNs, followed by RV. Both viruses induced expression of *Ifnb* and *Ifna4*, which encode type I IFNs known to be expressed early during antiviral responses [52, 53]. Five subtypes of *Ifna* were up-regulated by both PR8 and RV, while three *Ifna* subtypes were uniquely up-regulated by PR8 and only *Ifnab* was uniquely up-regulated by RV. Only PR8 induced expression of *Ifnar2*, which encodes the high affinity chain of the type I IFN α/β receptor [54]. This may allow for enhanced positive-feedback signaling and account for the larger number of IFN-induced genes up-regulated by PR8 infection.

Differential signaling through MDA-5 and RIG-I pathways may contribute to the differences in type I IFN responses by RV and PR8. Rhinoviruses and influenza A viruses are known to induce type I IFN responses through recognition by MDA-5 and RIG-I, respectively [55, 56]. Furthermore, both viruses are recognized by TLR3 in infected epithelial cells [55, 56]. However, TLR3 predominantly induces expression of pro-inflammatory genes, rather than type I IFN-dependent genes, during influenza A virus infection [55]. Zaritsky et al. have
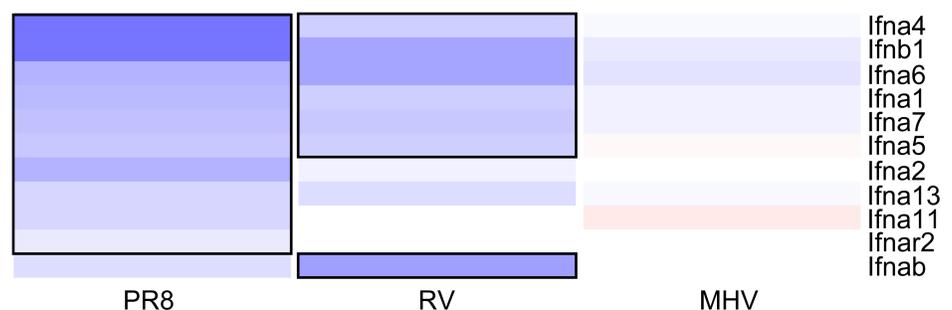
Fig 5. Differential expression of type I interferons and receptors. The $\log_2$-fold change compared to mock of up-regulated type I IFN cytokine and receptor genes. Gene names are shown to the right of each row and the color scale is the same as in Fig 4.

demonstrated that the type I IFN response to Sendai virus differs when cells are infected by different doses [57]. They further showed that these differences were mediated by differential signaling through the IFN α/β receptor, with robust signaling in uninfected cells. This supports our findings that PR8 induces expression of *Ifnar2* and additional type I IFN genes that are not up-regulated by RV (Fig 5).

None of the type I IFNs or receptors had significantly altered expression upon MHV infection (Fig 5), despite up-regulation of a modest number of IFN-stimulated genes (Fig 4). This could be due to IFN-independent expression of these genes, or induction by a type I IFN that was not represented on the microarray. Coronaviruses are notorious for being able to replicate within cells without triggering type I IFN responses, or delaying IFN induction until late in the replication cycle [36, 58–60]. Other studies have shown that the IFN response to MHV-1 is a critical determinant of susceptibility. Severe disease in A/J mice compared to C57Bl/6 mice correlates with lower type I IFNs detected in the lungs of A/J mice upon MHV-1 infection [6, 61]. Similarly, the expression of various type I IFNs in response to MHV-1 infection *in vitro* is cell line-dependent [61]. Because the cell line we used, LA4, was derived from the lungs of A/He mice, we would expect it to have a similar response as A/J mice. Thus the lack of type I IFNs induced by MHV-1 in LA4 cells *in vitro* corresponds with pathogenesis observed in A/J mice *in vivo*.

The finding that LA4 cells mount a stronger response to PR8 than RV or MHV infection may be due to differences in the viral recognition and signaling pathways used to detect these different viruses and amplification of the type I IFN response as discussed above. Alternatively, it could be due to the timing of our analysis. RV-infected cells have started dying by the 24 h time point (not shown), therefore expression of host genes may be declining by that time point. In contrast, coronaviruses are known to delay cellular responses to infection [62], so the 24 h time point may be too early to evaluate the innate response to MHV infection. Alternatively, the cells may detect MHV and up-regulate transcription of IFN response genes, but mRNA degradation would mask this process. By quantifying mRNA transcripts at two time points after viral infection, our study cannot distinguish between these possibilities.

RV1B induced a similar gene expression response in murine and human respiratory epithelial cells

One limitation of our study is the analysis of three viruses that do not share a natural host. MHV is a natural pathogen of mice and PR8 is a highly mouse-adapted strain of influenza A virus. However, RV1B is a human rhinovirus whose receptor is conserved between mice and humans. RV1B is increasingly being used in mouse studies [1–4, 63]. Despite the difference in host, we found similar changes to gene expression in murine cells as studies with RV1B in human cells [24]. Of the 24,204 and 12,438 genes represented on our mouse microarray and the human microarray chip used by Chen et al., respectively, 10,847 genes are shared. Using the same 2-fold increase in expression cut-off and restricting our list only to homologous human genes studied by Chen et al., we found that 196 mouse genes were up-regulated by RV1B infection. Comparing this list of 196 genes to the 48 up-regulated human genes identified by Chen et al., we found that 20 genes (S6 Table) were up-regulated by RV1B infection in both human and mouse cells. A chi-squared test confirmed the significance of this shared number of up-regulated genes (χ^2 = 431.7, d.f. = 1, $p<0.001$). Interestingly, all 20 of the shared genes we identified are involved in type I IFN responses. While far from identical, the similarity of the responses in the two cell types suggests conserved activation of type I IFN responses by these different hosts and supports the validity of a murine model for studying rhinovirus infections in humans.

Conclusions

Alveolar epithelial cells have a key role in alerting the immune system to infection by respiratory viruses and shaping immune responses [39, 64, 65]. As viruses from several different families all target respiratory epithelial cells, it is important to understand the similarities and differences in how these cells respond to a diverse set of viruses. A significant number of genes were up- or down-regulated in response to infection by three distinct viruses from different families. Genes that were associated with a shared response to the three viruses included those involved in defense against viruses and particularly genes induced by type I IFNs. However, there were differences in the timing, numbers of genes altered, and expression levels of these genes. This may reflect differences in viral replication cycles and signaling pathways that are activated by infection, which may reflect differences in pathogenesis of these viruses in murine models.

Supporting information

S1 Fig. Evaluation of LA4 cell susceptibility to infection by MHV, RV, and PR8. LA4 cells were inoculated with (A) 3 PFU/cell MHV, (C) 3 $TCID_{50}$/cell RV, or (E) 1 PFU/cell PR8, or were mock inoculated (B, D, F). Cells were fixed in 4% formaldehyde and permeabilized with Triton X100. (A, B) MHV infection was evaluated using a monoclonal antibody that recognizes the nucleocapsid protein (provided by Dr. Julian Leibowitz, Texas A&M University), followed by goat anti-mouse-555 (Invitrogen). (C, D) RV antigens were detected using RV1B antiserum (ATCC) and goat anti-guinea pig-488 (Rockland, Gilbertsville, PA). Goat antiserum NR-3148, which recognizes the hemagglutinin protein of PR8 (BEI Resources), and anti-goat-555 (Invitrogen) were used to detect PR8 infection. Nuclei were stained with DAPI and were photographed on a Nikon Eclipse Ti Epifluorescent Microscope with a Nikon DS-Qi2 camera and NIS Elements software (Nikon). (G) LA4 cells were inoculated with MHV, RV, or PR8, as described above and viral titers in the supernatant medium was analyzed by $TCID_{50}$ assays in MDCK (PR8), HeLa (RV), and 17cl1 (MHV) cell lines. Titers are the average and SEM of four replicate samples at each time point.
(PDF)

S2 Fig. RT-qPCR validation of candidate genes. LA4 cells were inoculated with virus using the same MOI's as for the microarray study and RNA was extracted at 24 h post-infection using Trizol (Ambion). RNA was converted to cDNA using random hexamers and Super-Script VILO (Invitrogen). Five genes with differential expression by microarray analysis were validated by qPCR analysis using SYBR green (PowerUP, Applied Biosystems) and the primer pairs listed in the figure on a StepOne Plus Instrument (Applied Biosystems). CT values from triplicate qPCR reactions were averaged and normalized to β-*actin* before calculating the fold change values of virus-infected samples vs. mock. Linear regression was used to compare fold change values between qPCR and microarray with removal of outliers (*) with Cook's distance > 0.5.
(PDF)

S3 Fig. Differential expression of type I interferon-induced genes. Genes with significantly up-regulated expression compared to mock at 24 h (see Fig 2) were used to query the Interferome v.2.01 database. Interferon-regulated genes were divided into functional groups and heat maps were generated using log_2-fold change values for each virus at 24 h compared to mock-inoculated controls. Heat maps of additional functional groups can be found in Fig 4. Gene names are indicated to the right of each row and statistically significant values are outlined in black.
(PDF)

S1 Table. Genes whose expression was significantly up-regulated by all three viruses compared to mock-inoculated cells. These genes were from the center of the Venn diagram in Fig 2A.
(XLSX)

S2 Table. Genes whose expression was significantly down-regulated by all three viruses compared to mock-inoculated cells. These genes were from the center of the Venn diagram in Fig 2B.
(XLSX)

S3 Table. Signature genes for PR8. These genes were significantly different in PR8 infection compared to mock, RV, and MHV.
(XLSX)

S4 Table. Signature genes for RV. These genes were significantly different in RV infection compared to mock, PR8, and MHV.
(XLSX)

S5 Table. Signature genes for MHV. These genes were significantly different in MHV infection compared to mock, RV, and PR8.
(XLSX)

S6 Table. Genes up-regulated by RV in both murine and human cells. These genes were identified to be up-regulated in our study by RV1B in murine cells and also were found by Chen et al. (23) to be up-regulated by RV1B in human cells.
(XLSX)

Acknowledgments

Author Contributions

Conceptualization: TAM CRM.

Data curation: CRM BJR JTV TAM.

Formal analysis: CRM BJR JTV.

Funding acquisition: TAM CRM.

Investigation: TAM AJG.

Methodology: TAM AJG.

Project administration: TAM.

Resources: TAM.

Visualization: CRM BJR JTV AJG TAM.

Writing – original draft: TAM.

Writing – review & editing: TAM BJR CRM JTV AJG.

References

1. Bartlett NW, Walton RP, Edwards MR, Aniscenko J, Caramori G, Zhu J, et al. Mouse models of rhinovirus-induced disease and exacerbation of allergic airway inflammation. Nat Med. 2008; 14(2):199–204. Epub 2008/02/05. https://doi.org/10.1038/nm1713 PMID: 18246079

2. Lee SB, Song JA, Choi GE, Kim HS, Jang YJ. Rhinovirus infection in murine chronic allergic rhinosinusitis model. Int Forum Allergy Rhinol. 2016; 6(11):1131–8. https://doi.org/10.1002/alr.21805 PMID: 27348296

3. Nagarkar DR, Wang Q, Shim J, Zhao Y, Tsai WC, Lukacs NW, et al. CXCR2 is required for neutrophilic airway inflammation and hyperresponsiveness in a mouse model of human rhinovirus infection. J Immunol. 2009; 183(10):6698–707. PubMed Central PMCID: PMCPMC2952174. https://doi.org/10.4049/jimmunol.0900298 PMID: 19864593

4. Newcomb DC, Sajjan US, Nagarkar DR, Wang Q, Nanua S, Zhou Y, et al. Human rhinovirus 1B exposure induces phosphatidylinositol 3-kinase-dependent airway inflammation in mice. Am J Respir Crit Care Med. 2008; 177(10):1111–21. Epub 2008/02/16. PubMed Central PMCID: PMC2383993. https://doi.org/10.1164/rccm.200708-1243OC PMID: 18276942

5. Wang Q, Miller DJ, Bowman ER, Nagarkar DR, Schneider D, Zhao Y, et al. MDA5 and TLR3 initiate pro-inflammatory signaling pathways leading to rhinovirus-induced airways inflammation and hyperresponsiveness. PLoS Pathog. 2011; 7(5):e1002070. PubMed Central PMCID: PMCPMC3102730. https://doi.org/10.1371/journal.ppat.1002070 PMID: 21637773

6. De Albuquerque N, Baig E, Ma X, Zhang J, He W, Rowe A, et al. Murine hepatitis virus strain 1 produces a clinically relevant model of severe acute respiratory syndrome in A/J mice. J Virol. 2006; 80 (21):10382–94. https://doi.org/10.1128/JVI.00747-06 PMID: 17041219

7. Leibowitz JL, Srinivasa R, Williamson ST, Chua MM, Liu M, Wu S, et al. Genetic determinants of mouse hepatitis virus strain 1 pneumovirulence. J Virol. 2010; 84(18):9278–91. Epub 2010/07/16. PubMed Central PMCID: PMC2937641. https://doi.org/10.1128/JVI.00330-10 PMID: 20631137

8. Khanolkar A, Hartwig SM, Haag BA, Meyerholz DK, Harty JT, Varga SM. Toll-like receptor 4 deficiency increases disease and mortality after mouse hepatitis virus type 1 infection of susceptible C3H mice. J Virol. 2009; 83(17):8946–56. Epub 2009/06/26. PubMed Central PMCID: PMC2738158. https://doi.org/10.1128/JVI.01857-08 PMID: 19553337

9. Kebaabetswe LP, Haick AK, Miura TA. Differentiated phenotypes of primary murine alveolar epithelial cells and their susceptibility to infection by respiratory viruses. Virus Res. 2013; 175(2):110–9. Epub 2013/05/04. PubMed Central PMCID: PMC3683362. https://doi.org/10.1016/j.virusres.2013.04.008 PMID: 23639425

10. Srivastava B, Blazejewska P, Hessmann M, Bruder D, Geffers R, Mauel S, et al. Host genetic background strongly influences the response to influenza a virus infections. PLoS One. 2009; 4(3):e4857. Epub 2009/03/19. PubMed Central PMCID: PMC2654507. https://doi.org/10.1371/journal.pone.0004857 PMID: 19293935

11. Alberts R, Srivastava B, Wu H, Viegas N, Geffers R, Klawonn F, et al. Gene expression changes in the host response between resistant and susceptible inbred mouse strains after influenza A infection. Microbes and infection / Institut Pasteur. 2010; 12(4):309–18.

12. Blazejewska P, Koscinski L, Viegas N, Anhlan D, Ludwig S, Schughart K. Pathogenicity of different PR8 influenza A virus variants in mice is determined by both viral and host factors. Virology. 2011; 412 (1):36–45. Epub 2011/01/25. https://doi.org/10.1016/j.virol.2010.12.047 PMID: 21256531

13. Fukushi M, Ito T, Oka T, Kitazawa T, Miyoshi-Akiyama T, Kirikae T, et al. Serial histopathological examination of the lungs of mice infected with influenza A virus PR8 strain. PLoS One. 2011; 6(6):e21207. Epub 2011/06/28. PubMed Central PMCID: PMC3118813. https://doi.org/10.1371/journal.pone.0021207 PMID: 21701593

14. Kebaabetswe LP, Haick AK, Gritsenko MA, Fillmore TL, Chu RK, Purvine SO, et al. Proteomic analysis reveals down-regulation of surfactant protein B in murine type II pneumocytes infected with influenza A

virus. Virology. 2015; 483:96–107. PubMed Central PMCID: PMCPMC4516596. https://doi.org/10.1016/j.virol.2015.03.045 PMID: 25965799

15. Tate MD, Schilter HC, Brooks AG, Reading PC. Responses of mouse airway epithelial cells and alveolar macrophages to virulent and avirulent strains of influenza A virus. Viral immunology. 2011; 24(2):77–88. Epub 2011/04/01. https://doi.org/10.1089/vim.2010.0118 PMID: 21449718

16. Stoner GD, Hallman M, Troxell MC. Lecithin biosynthesis in a clonal line of lung adenoma cells with type II alveolar cell properties. Experimental and molecular pathology. 1978; 29(1):102–14. PMID: 581072

17. Tuthill TJ, Papadopoulos NG, Jourdan P, Challinor LJ, Sharp NA, Plumpton C, et al. Mouse respiratory epithelial cells support efficient replication of human rhinovirus. J Gen Virol. 2003; 84(Pt 10):2829–36. Epub 2003/09/19. https://doi.org/10.1099/vir.0.19109-0 PMID: 13679617

18. Szretter KJ, Balish AL, Katz JM. Influenza: propagation, quantification, and storage. Current protocols in microbiology. 2006;Chapter 15:Unit 15G 1.

19. Sturman LS, Takemoto KK. Enhanced growth of a murine coronavirus in transformed mouse cells. Infection and immunity. 1972; 6(4):501–7. Epub 1972/10/01. PubMed Central PMCID: PMC422565. PMID: 4564284

20. Rosenblum EB, Poorten TJ, Joneson S, Settles M. Substrate-specific gene expression in Batrachochytrium dendrobatidis, the chytrid pathogen of amphibians. PLoS ONE. 2012; 7(11):e49924. Epub 2012/11/28. PubMed Central PMCID: PMC3502224. https://doi.org/10.1371/journal.pone.0049924 PMID: 23185485

21. Carvalho BS, Irizarry RA. A framework for oligonucleotide microarray preprocessing. Bioinformatics. 2010; 26(19):2363–7. PubMed Central PMCID: PMCPMC2944196. https://doi.org/10.1093/bioinformatics/btq431 PMID: 20688976

22. Benjamini Y, Hochberg Y. Controlling the False Discovery Rate—a Practical and Powerful Approach to Multiple Testing. J Roy Stat Soc B Met. 1995; 57(1):289–300.

23. Rusinova I, Forster S, Yu S, Kannan A, Masse M, Cumming H, et al. Interferome v2.0: an updated database of annotated interferon-regulated genes. Nucleic acids research. 2013; 41:D1040–6. PubMed Central PMCID: PMC3531205. https://doi.org/10.1093/nar/gks1215 PMID: 23203888

24. Chen Y, Hamati E, Lee PK, Lee WM, Wachi S, Schnurr D, et al. Rhinovirus induces airway epithelial gene expression through double-stranded RNA and IFN-dependent pathways. Am J Respir Cell Mol Biol. 2006; 34(2):192–203. PubMed Central PMCID: PMCPMC2644182. https://doi.org/10.1165/rcmb.2004-0417OC PMID: 16210696

25. Eppig JT, Blake JA, Bult CJ, Kadin JA, Richardson JE, Mouse Genome Database G. The Mouse Genome Database (MGD): facilitating mouse as a model for human biology and disease. Nucleic acids research. 2015; 43:D726–36. PubMed Central PMCID: PMCPMC4384027. https://doi.org/10.1093/nar/gku967 PMID: 25348401

26. Raaben M, Groot Koerkamp MJ, Rottier PJ, de Haan CA. Mouse hepatitis coronavirus replication induces host translational shutoff and mRNA decay, with concomitant formation of stress granules and processing bodies. Cellular microbiology. 2007; 9(9):2218–29. https://doi.org/10.1111/j.1462-5822.2007.00951.x PMID: 17490409

27. Josset L, Menachery VD, Gralinski LE, Agnihothram S, Sova P, Carter VS, et al. Cell host response to infection with novel human coronavirus EMC predicts potential antivirals and important differences with SARS coronavirus. MBio. 2013; 4(3):e00165–13. PubMed Central PMCID: PMCPMC3663187. https://doi.org/10.1128/mBio.00165-13 PMID: 23631916

28. Sims AC, Tilton SC, Menachery VD, Gralinski LE, Schafer A, Matzke MM, et al. Release of severe acute respiratory syndrome coronavirus nuclear import block enhances host transcription in human lung cells. J Virol. 2013; 87(7):3885–902. PubMed Central PMCID: PMCPMC3624188. https://doi.org/10.1128/JVI.02520-12 PMID: 23365422

29. Kamitani W, Narayanan K, Huang C, Lokugamage K, Ikegami T, Ito N, et al. Severe acute respiratory syndrome coronavirus nsp1 protein suppresses host gene expression by promoting host mRNA degradation. Proc Natl Acad Sci U S A. 2006; 103(34):12885–90. Epub 2006/08/17. https://doi.org/10.1073/pnas.0603144103 PMID: 16912115

30. Amineva SP, Aminev AG, Palmenberg AC, Gern JE. Rhinovirus 3C protease precursors 3CD and 3CD' localize to the nuclei of infected cells. J Gen Virol. 2004; 85(Pt 10):2969–79. https://doi.org/10.1099/vir.0.80164-0 PMID: 15448360

31. Bochkov YA, Hanson KM, Keles S, Brockman-Schneider RA, Jarjour NN, Gern JE. Rhinovirus-induced modulation of gene expression in bronchial epithelial cells from subjects with asthma. Mucosal immunology. 2010; 3(1):69–80. PubMed Central PMCID: PMCPMC2884103. https://doi.org/10.1038/mi.2009.109 PMID: 19710636

32. Bosco A, Wiehler S, Proud D. Interferon regulatory factor 7 regulates airway epithelial cell responses to human rhinovirus infection. BMC genomics. 2016; 17:76. PubMed Central PMCID: PMCPMC4727386. https://doi.org/10.1186/s12864-016-2405-z PMID: 26810609

33. Kim TK, Bheda-Malge A, Lin Y, Sreekrishna K, Adams R, Robinson MK, et al. A systems approach to understanding human rhinovirus and influenza virus infection. Virology. 2015; 486:146–57. https://doi.org/10.1016/j.virol.2015.08.014 PMID: 26437235

34. Proud D, Turner RB, Winther B, Wiehler S, Tiesman JP, Reichling TD, et al. Gene expression profiles during in vivo human rhinovirus infection: insights into the host response. Am J Respir Crit Care Med. 2008; 178(9):962–8. https://doi.org/10.1164/rccm.200805-670OC PMID: 18658112

35. Ioannidis I, McNally B, Willette M, Peeples ME, Chaussabel D, Durbin JE, et al. Plasticity and virus specificity of the airway epithelial cell immune response during respiratory virus infection. J Virol. 2012; 86(10):5422–36. PubMed Central PMCID: PMCPMC3347264. https://doi.org/10.1128/JVI.06757-11 PMID: 22398282

36. Menachery VD, Eisfeld AJ, Schafer A, Josset L, Sims AC, Proll S, et al. Pathogenic influenza viruses and coronaviruses utilize similar and contrasting approaches to control interferon-stimulated gene responses. MBio. 2014; 5(3):e01174–14. PubMed Central PMCID: PMCPMC4030454. https://doi.org/10.1128/mBio.01174-14 PMID: 24846384

37. Wang J, Nikrad MP, Phang T, Gao B, Alford T, Ito Y, et al. Innate immune response to influenza A virus in differentiated human alveolar type II cells. Am J Respir Cell Mol Biol. 2011; 45(3):582–91. Epub 2011/01/18. PubMed Central PMCID: PMC3175576. https://doi.org/10.1165/rcmb.2010-0108OC PMID: 21239608

38. Lee SM, Chan RW, Gardy JL, Lo CK, Sihoe AD, Kang SS, et al. Systems-level comparison of host responses induced by pandemic and seasonal influenza A H1N1 viruses in primary human type I-like alveolar epithelial cells in vitro. Respir Res. 2010; 11:147. PubMed Central PMCID: PMCPMC2988725. https://doi.org/10.1186/1465-9921-11-147 PMID: 21029402

39. Stegemann-Koniszewski S, Jeron A, Gereke M, Geffers R, Kroger A, Gunzer M, et al. Alveolar Type II Epithelial Cells Contribute to the Anti-Influenza A Virus Response in the Lung by Integrating Pathogen- and Microenvironment-Derived Signals. MBio. 2016; 7(3):e00276–16. PubMed Central PMCID: PMCPMC4959657. https://doi.org/10.1128/mBio.00276-16 PMID: 27143386

40. Le Goffic R, Balloy V, Lagranderie M, Alexopoulou L, Escriou N, Flavell R, et al. Detrimental contribution of the Toll-like receptor (TLR)3 to influenza A virus-induced acute pneumonia. PLoS Pathog. 2006; 2 (6):e53. Epub 2006/06/23. PubMed Central PMCID: PMC1475659. https://doi.org/10.1371/journal.ppat.0020053 PMID: 16789835

41. Clarke DL, Davis NH, Majithiya JB, Piper SC, Lewis A, Sleeman MA, et al. Development of a mouse model mimicking key aspects of a viral asthma exacerbation. Clin Sci (Lond). 2014; 126(8):567–80.

42. Christiansen SC, Eddleston J, Bengtson SH, Jenkins GR, Sarnoff RB, Turner RB, et al. Experimental rhinovirus infection increases human tissue kallikrein activation in allergic subjects. Int Arch Allergy Immunol. 2008; 147(4):299–304. https://doi.org/10.1159/000144037 PMID: 18617749

43. Naclerio RM, Proud D, Lichtenstein LM, Kagey-Sobotka A, Hendley JO, Sorrentino J, et al. Kinins are generated during experimental rhinovirus colds. J Infect Dis. 1988; 157(1):133–42. PMID: 2447198

44. Hewson CA, Haas JJ, Bartlett NW, Message SD, Laza-Stanca V, Kebadze T, et al. Rhinovirus induces MUC5AC in a human infection model and in vitro via NF-kappaB and EGFR pathways. Eur Respir J. 2010; 36(6):1425–35. https://doi.org/10.1183/09031936.00026910 PMID: 20525715

45. van der Meer Y, Snijder EJ, Dobbe JC, Schleich S, Denison MR, Spaan WJ, et al. Localization of mouse hepatitis virus nonstructural proteins and RNA synthesis indicates a role for late endosomes in viral replication. J Virol. 1999; 73(9):7641–57. PubMed Central PMCID: PMCPMC104292. PMID: 10438855

46. Sims AC, Ostermann J, Denison MR. Mouse hepatitis virus replicase proteins associate with two distinct populations of intracellular membranes. J Virol. 2000; 74(12):5647–54. PubMed Central PMCID: PMCPMC112052. PMID: 10823872

47. Kindler E, Gil-Cruz C, Spanier J, Li Y, Wilhelm J, Rabouw HH, et al. Early endonuclease-mediated evasion of RNA sensing ensures efficient coronavirus replication. PLoS Pathog. 2017; 13(2):e1006195. PubMed Central PMCID: PMCPMC5310923. https://doi.org/10.1371/journal.ppat.1006195 PMID: 28158275

48. Zust R, Cervantes-Barragan L, Habjan M, Maier R, Neuman BW, Ziebuhr J, et al. Ribose 2'-O-methylation provides a molecular signature for the distinction of self and non-self mRNA dependent on the RNA sensor Mda5. Nature immunology. 2011; 12(2):137–43. PubMed Central PMCID: PMCPMC3182538. https://doi.org/10.1038/ni.1979 PMID: 21217758

49. Khanolkar A, Hartwig SM, Haag BA, Meyerholz DK, Epping LL, Haring JS, et al. Protective and pathologic roles of the immune response to mouse hepatitis virus type 1: implications for severe acute

respiratory syndrome. J Virol. 2009; 83(18):9258–72. Epub 2009/07/03. PubMed Central PMCID: PMC2738266. https://doi.org/10.1128/JVI.00355-09 PMID: 19570864

50. Khanolkar A, Fulton RB, Epping LL, Pham NL, Tifrea D, Varga SM, et al. T cell epitope specificity and pathogenesis of mouse hepatitis virus-1-induced disease in susceptible and resistant hosts. J Immunol. 2010; 185(2):1132–41. PubMed Central PMCID: PMCPMC2897948. https://doi.org/10.4049/jimmunol.0902749 PMID: 20554960

51. van Pesch V, Lanaya H, Renauld JC, Michiels T. Characterization of the murine alpha interferon gene family. J Virol. 2004; 78(15):8219–28. PubMed Central PMCID: PMCPMC446145. https://doi.org/10.1128/JVI.78.15.8219-8228.2004 PMID: 15254193

52. Maniatis T, Goodbourn S, Fischer JA. Regulation of inducible and tissue-specific gene expression. Science. 1987; 236(4806):1237–45. PMID: 3296191

53. Marie I, Durbin JE, Levy DE. Differential viral induction of distinct interferon-alpha genes by positive feedback through interferon regulatory factor-7. The EMBO journal. 1998; 17(22):6660–9. PubMed Central PMCID: PMCPMC1171011. https://doi.org/10.1093/emboj/17.22.6660 PMID: 9822609

54. de Weerd NA, Nguyen T. The interferons and their receptors—distribution and regulation. Immunology and cell biology. 2012; 90(5):483–91. https://doi.org/10.1038/icb.2012.9 PMID: 22410872

55. Le Goffic R, Pothlichet J, Vitour D, Fujita T, Meurs E, Chignard M, et al. Cutting Edge: Influenza A virus activates TLR3-dependent inflammatory and RIG-I-dependent antiviral responses in human lung epithelial cells. J Immunol. 2007; 178(6):3368–72. PMID: 17339430

56. Wang Q, Nagarkar DR, Bowman ER, Schneider D, Gosangi B, Lei J, et al. Role of double-stranded RNA pattern recognition receptors in rhinovirus-induced airway epithelial cell responses. J Immunol. 2009; 183(11):6989–97. PubMed Central PMCID: PMCPMC2920602. https://doi.org/10.4049/jimmunol.0901386 PMID: 19890046

57. Zaritsky LA, Bedsaul JR, Zoon KC. Virus Multiplicity of Infection Affects Type I Interferon Subtype Induction Profiles and Interferon-Stimulated Genes. J Virol. 2015; 89(22):11534–48. PubMed Central PMCID: PMCPMC4645643. https://doi.org/10.1128/JVI.01727-15 PMID: 26355085

58. Rose KM, Weiss SR. Murine Coronavirus Cell Type Dependent Interaction with the Type I Interferon Response. Viruses. 2009; 1(3):689–712. PubMed Central PMCID: PMCPMC2835314. https://doi.org/10.3390/v1030689 PMID: 20221421

59. Versteeg GA, Bredenbeek PJ, van den Worm SH, Spaan WJ. Group 2 coronaviruses prevent immediate early interferon induction by protection of viral RNA from host cell recognition. Virology. 2007; 361(1):18–26. Epub 2007/02/24. https://doi.org/10.1016/j.virol.2007.01.020 PMID: 17316733

60. Zhou H, Perlman S. Mouse hepatitis virus does not induce Beta interferon synthesis and does not inhibit its induction by double-stranded RNA. J Virol. 2007; 81(2):568–74. Epub 2006/11/03. https://doi.org/10.1128/JVI.01512-06 PMID: 17079305

61. Baig E, Fish EN. Distinct signature type I interferon responses are determined by the infecting virus and the target cell. Antivir Ther. 2008; 13(3):409–22. PMID: 18572754

62. Yoshikawa T, Hill TE, Yoshikawa N, Popov VL, Galindo CL, Garner HR, et al. Dynamic innate immune responses of human bronchial epithelial cells to severe acute respiratory syndrome-associated coronavirus infection. PLoS One. 2010; 5(1):e8729. Epub 2010/01/22. https://doi.org/10.1371/journal.pone.0008729 PMID: 20090954

63. Han M, Chung Y, Young Hong J, Rajput C, Lei J, Hinde JL, et al. Toll-like receptor 2-expressing macrophages are required and sufficient for rhinovirus-induced airway inflammation. The Journal of allergy and clinical immunology. 2016; 138(6):1619–30. https://doi.org/10.1016/j.jaci.2016.01.037 PMID: 27084403

64. Miura TA, Holmes KV. Host-pathogen interactions during coronavirus infection of primary alveolar epithelial cells. J Leukoc Biol. 2009; 86(5):1145–51. https://doi.org/10.1189/jlb.0209078 PMID: 19638499

65. Rzepka JP, Haick AK, Miura TA. Virus-infected alveolar epithelial cells direct neutrophil chemotaxis and inhibit their apoptosis. Am J Respir Cell Mol Biol. 2012; 46(6):833–41. Epub 2012/02/09. https://doi.org/10.1165/rcmb.2011-0230OC PMID: 22312020